Hybrid Genetic Optimization and Statistical Model-Based Approach for the Classification of Shadow Shapes in Sonar Imagery

Max Mignotte, Christophe Collet, Patrick Pérez, and Patrick Bouthemy

Abstract—We present an original statistical classification method using a deformable template model to separate natural objects from man-made objects in an image provided by a high resolution sonar. A prior knowledge of the manufactured object shadow shape is captured by a prototype template, along with a set of admissible linear transformations, to take into account the shape variability. Then, the classification problem is defined as a two-step process. First, the detection problem of a region of interest in the input image is stated as the minimization of a cost function. Second, the value of this function at convergence allows one to determine whether the desired object is present or not in the sonar image. The energy minimization problem is tackled using relaxation techniques. In this context, we compare the results obtained with a deterministic relaxation technique (a gradient-based algorithm) and two stochastic relaxation methods: Simulated Annealing (SA) and a hybrid Genetic Algorithm (GA). This latter method has been successfully tested on real and synthetic sonar images, yielding very promising results.

Index Terms—Deformable template, objective function, simulated annealing, gradient-based algorithm, genetic optimization, shape recognition, sonar imagery.

1 Introduction

Due to their high resolution, existing sonars can detect every object lying on the sea-bed. Each object can be identified efficiently thanks to an analysis of its associated cast shadow (arising from the lack of acoustic reverberation behind the object). However, since the amount and size of acquired images is huge, the exploitation of the collected data has to be achieved with an automatic processing chain. The goal is to be able to detect, in the context of our application (i.e., mine detection and neutralization, underwater wreckage research, submarine rescue...) manufactured objects lying on the sea-bed. On large sea floor areas (typically 1,000 meters by 200 meters), the goal is to find an object of size smaller than 6 meters by 3 meters. Immediately after such a detection, other means are deployed in order to confirm the detection and eventually destroy the threat. It is our applicative context. The proposed method may also be efficiently exploited to detect and to localize cylindrical or spherical objects lying on the sea-floor. Unfortunately, confidentiality reasons prevent us from providing too much information on the application. The approach presented in this paper allows us to efficiently distinguish natural objects from such manufactured objects lying on the sea-bed. The whole paper is presented with this intention.

- *M. Mignotte and C. Collet are with the Groupe de Traitement du Signal, Ecole Navale, BP 600, 29240 Brest-Naval France. E-mail: collet@poseidon.ecole-navale.fr.*
- *P. Pérez and P. Bouthemy are with IRISA/INRIA, Campus Universitaire de Beaulieu, 35042 Rennes cedex, France. E-mail: {perez, bouthemy}@irisa.fr.*

Manuscript received 26 Feb. 1998; accepted 13 Oct. 1999. Recommended for acceptance by J. Connell. For information on obtaining reprints of this article, please send e-mail to: tpami@computer.org, and reference IEEECS Log Number 107797.

In computer vision, pattern recognition issues are often cast as a search problem in some appropriate feature space. In that prospect, a classical and generally used recognition approach in sonar imagery consists of using a presegmented sonar image and associating, for each detected cast shadow shape, a set of appropriate geometrical, spectral, or statistical features. The aim is to represent the (shadow) shape with a relevant parameter vector providing maximal information about the extracted shadow. Afterward, this parameter vector is usually exploited as an input of a supervised classifier (Bayesian classifiers, K-nearest neighbors, or multilayer perceptron, ...) [1], [2]. The classification problem is reduced to recover from a database the occurrence that is the more similar to the analyzed one. This method is appealing and has been widely used in pattern recognition applications. Nevertheless, it requires that the training set be large enough to ensure an efficient learning stage. Besides, the efficiency of this technique depends on the feature extraction step for which there are no general rules to determine the optimal number of parameters and the discriminant characteristics of each of them. Note that this method cannot be used efficiently when the extracted shadow shape is partly merged with an other object shadow. In our application, it is often the case that cast shadow shapes are altered by the shadow of ridges of sand, dunes, or pebbles [3].

Contrary to the cast shadow of a natural object, the one of a manufactured object has a regular and/or geometrical shape easily identifiable. Bayesian statistical theory is a convenient way of taking this a priori information into consideration. This paradigm in image analysis is quite popular and has been successfully applied for image segmentation [4], [5], image restoration [6] (with a local prior model), or shape matching with deformable template-

based methods (with a global prior model) [7], [8]. Laksmanan and Grimmer [9], for example, have used a parametric template model to locate the road boundary in radar images where the two straight, parallel edges of a road are parameterized. Then, the edge detection problem is formulated as a Bayesian optimization problem using a physics-based model of the radar imaging process. A similar approach for shape matching is proposed by Jain et al. [10], [11] which combines, in the same manner, both the available knowledge of the shape properties (as prior model) and an observation model (as likelihood model). One such method can be efficiently used for the classification of the cast shadow of each object lying on the sea-bed and to more precisely distinguish natural objects from man-made objects in sonar imagery. In this way, we define a prototype template and a set of admissible linear transformations to take into account the shape variability of the object class to be detected. Also, we define a joint Probability Density Function (PDF) which expresses the dependence between the observed image and the deformed template. Then, the detection problem of an object class is stated as the estimation of the deformation parameters of the template that maximize the posterior PDF. This maximization problem is equivalent to the minimization of a nonconcave (usually complex with many local extrema) objective function.

In [10], gradient-based methods are used for the energy minimization of this function. These methods have the disadvantage of requiring good initial parameter estimates (i.e., a proper initialization of the template), otherwise, they will converge toward bad local minima. Stochastic methods based on Simulated Annealing (SA) [12], [13] have the capability of avoiding local minima and no human interaction is required to initialize the model. However, one of the major drawbacks of this procedure is its high computational load. Hereafter, we show that an alternate approach consists of using a genetic exploration of the parameter space.

The main contribution of this paper lies in the use of deformable model to classify objects in sonar imagery. This appears as an interesting alternative to feature-based matching methods and it is efficient in the case of complex background and/or occlusion phenomena between several cast shadows. We propose an appropriate energy function that differs from previously published works. This energy utilizes the information given by an unsupervised Markovian segmentation of the input sonar image [5] and integrates both region homogeneity and edge information. Finally, we introduce a computationally efficient global optimization method to solve the minimization problem. This method is based on a stochastic search method using a genetic exploration of the parameter search space combined with a steepest ascent procedure and a cooling temperature schedule. In such a context, we will show that the use of Genetic Algorithm (GA) leads to better performance than other stochastic methods (such as simulated annealing) or deterministic relaxation techniques like gradient-based algorithm.

This paper is organized as follows: Sections 2 and 3 present the template modeling and the energy-based extraction of template occurrences from data and the classification of extracted shapes. The optimization using gradient-based algorithm, simulated annealing, or GA is described in Section 4. In Section 5, we report some detection/classification results on real and synthetic sonar images. In this context, advantages of GA over the other optimization methods are discussed. Section 6 contains concluding remarks.

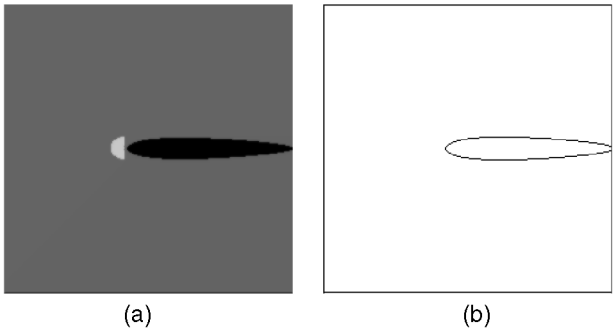

Fig. 1. (a) Cast shadow and echo associated with a spherical object, synthesized with a ray tracing procedure. (b) Associated prototype template.

2 Template Representation

Contour-based modeling is a generic tool for shape matching. It can be applied to objects of different shapes by defining different prototype templates.

In sonar imagery, the first goal of the classification step is to automatically separate natural objects from man-made objects. This low-level classification step in two classes is based on the following a priori information: Contrary to natural objects, a manufactured object is mainly composed of elements with simple and regular geometrical shape. For this reason, their cast shadow present geometric properties and exhibit straight lines as contours in the case of wrecks, pipe-lines, etc. In particular, the cast shadow of a cylindrical or cubic object is a perfect parallelogram. Therefore, we simply define the corresponding prototype template as a parallelogram characterized by its four vertices. For a different application, however, we have to detect spherical objects lying on the sea-bed. In this case, the associated cast shadow has a typical shape whose representation can easily be defined by a set of n points manually selected or equally sampled which approximate its outline. A cubic B-spline shape representation involving these n control points corresponding to "landmarks" is then defined. The outline of the spherical object cast shadow used to build the prototype can either be obtained from a real scene or synthesized (see Fig. 1). The latter way of modeling objects has been widely considered in the object recognition literature and, particularly, in the active contour approach [14]. Such a scheme captures the global structure of a shape without specifying a parametric form for each class of shapes.

The prototype template, denoted γ_0, does not describe the possible instances of the shapes to be detected for a class of objects. In order to take into account the variability of the considered object class, we introduce a set of admissible

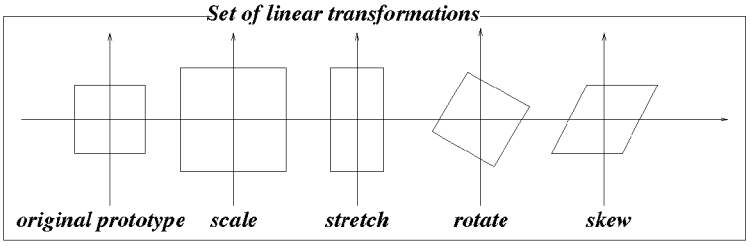

Fig. 2. Considered linear transformations in $\mathbb{R}^2$ for the original prototype associated with the cast shadow of a manufactured object with a regular shape.

linear transformations on γ_0. Let γ_θ be a deformed version of the original prototype γ_0 according to a affine transformation with parameters vector θ. In the case of our first parametric template (used to detect manufactured object), these deformations involve translation, scaling, rotation, stretching, and skewing [15] of the template, as shown in Fig. 2. Corresponding transformations are given by:

$$A_s = \begin{pmatrix} s & 0 \\ 0 & s \end{pmatrix} \qquad A_\alpha = \begin{pmatrix} cos\alpha & -sin\alpha \\ sin\alpha & cos\alpha \end{pmatrix}$$
$$A_t = \begin{pmatrix} 1 & 0 \\ 0 & t \end{pmatrix} \qquad A_u = \begin{pmatrix} 1 & u \\ 0 & 1 \end{pmatrix}$$

with s, t, u, and α being, respectively, the scale, stretch, and skew parameters and the angle of rotation.

Due to spherical symmetry, the spherical object cast shadow is symmetric relative to the sonar beam direction. Therefore, the only considered transformations are translation, scaling, and stretching for this template (see Fig. 3).

Otherwise, parameters of the translation and the scale transformation are actually constrained by the size of the subimage. Translation parameter (in the x or y axis direction), as well as scale, stretch, and skew parameters, are constrained such that the template stays, at least partially, within the subimage.

In order to correctly detect and classify cast shadows that are partly outside the subimage, we have to partition the input sonar image of large size (typically 6,000 by 2,000 pels) into small *overlapping* subimages (256 by 256 pels) whose size is a function of the template size we are looking for (typically, 30 by 60 pels). The detection-classification method presented in the next part then has to be used for each overlapping subimage.

3 Map Detection

A common problem in sonar images are the artifacts caused by the speckle noise effect, which leads to a loss of signal and a very poor quality of the object boundaries [16]. That is why the joint model we propose does not directly use the input image (i.e., the gray levels themselves) or some image gradient measure (as proposed in [10]) in order to recover the contour of each object. In our approach, we use the result of an unsupervised two-class Markovian segmentation of the input sonar image [5]. It provides a binary map $x = \{x_s, s \in S\}$, where $x_s = e_0$ for *shadow* areas and $x_s = e_1$ for *reverberation* areas. This allows us to take into account the observed measurements along regions contours, but also the gray-level homogeneity information inside and outside delimited regions. The detection is based on an objective function ϵ measuring how well a given instance of deformed template γ_θ fits the content of segmented image x. From a probabilistic point of view, $\epsilon(\theta, x)$ defines the joint model through the Gibbs distribution:

$$P_{\Theta,X}(\theta, x) = \frac{1}{Z}\exp\{-\epsilon(\theta, x)\}, \tag{1}$$

where Θ is the random vector of parameters and Z is a normalizing constant.

3.1 Joint Model

The posterior distribution deduced from (1):

$$P_{\Theta/X}(\theta/x) = \frac{1}{Z_x}\exp\{-\epsilon(\theta, x)\} \tag{2}$$

provides the probability of a given template given the segmented image. $\epsilon(\theta, x)$ represents a measurement of the similarity between the deformed template and the object present in the image. The energy function $\epsilon(\theta, x)$ is composed of two terms as explained below:

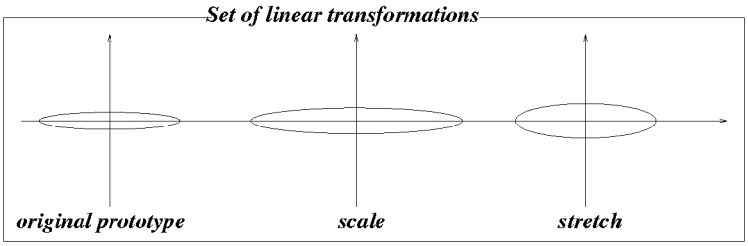

Fig. 3. Considered linear transformations in $\mathbb{R}^2$ for the original prototype associated with the cast shadow of a spherically shaped object.

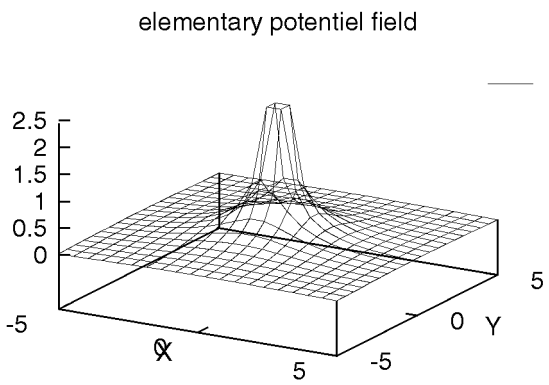

Fig. 4. Elementary potential field created by a site associated with an edge of a detected shadow region in x ($\sigma = 1$).

Edge energy: Let S' be the set of 1-labeled pixels in a binarized high-pass filtered version of the segmented sonar image x in two classes (i.e., S' represents the set of edges associated to detected cast shadows). The deformable template is attracted and aligned to the salient contours of each object *via* an edge potential field defined as follows: Each site $s_0 \in S'$ associated to an edge of a detected shadow region in S' creates an elementary potential field $\phi_{s_0}(r)$ such as:

$$\phi_{s_0}(r) = \frac{1}{r}\exp\Big(-\frac{r}{\sigma}\Big), \tag{3}$$

where r ($r \neq 0$) is the distance to the pixel s_0. Fig. 4 shows an example of this elementary potential field. The different edges in S' create a potential field $\Phi_{S'}(t)$, given by the total sum of the different elementary potential fields $\phi_{s_0}(r)$:

$$\Phi_{S'}(t) = \inf\left\{\sum_{s\in S'}\phi_s(d(s,t)), 1\right\} \qquad \forall t \in S' \tag{4}$$

with $d(s,t)$ the distance between pixels s and t. In fact, this potential field induces a smooth version of the edge image in which a site close to an edge will get a potential value close to 1, as illustrated in Fig. 5. The degree of smoothness can be controlled by parameter σ. This edge potential field induces an energy function that relates a deformed template γ_θ to the edges associated to each detected object in the input image:

$$\epsilon_c(\theta, x) = -\ln\left\{\frac{1}{N_{\gamma_\theta}}\sum_{s\in\gamma_\theta}\Phi_{S'}(s)\right\} \quad \geq 0, \tag{5}$$

where the summation is over all the N_{γ_θ} pixels on the deformed template γ_θ and the logarithm function is used to increase the range of the energy function ϵ_c. This function attains its minimum value when the contour of the deformed template coincides exactly with the underlying image edges.

Region homogeneity energy: This energy term aims at placing the inside of the deformed template in a region classified as shadow by the segmentation procedure:

$$\epsilon_r(\theta, x) = -\ln\left\{\frac{1}{N_{\gamma_\theta^\bullet}}\sum_{s\in\gamma_\theta^\bullet}\delta(x_s, e_0)\right\} \quad \geq 0, \tag{6}$$

where $\gamma_\theta^\bullet$ and $N_{\gamma_\theta^\bullet}$ represent the set of pixels and the number of pixels inside the region delimited by γ_θ and $\delta(.)$ is the Kronecker delta function. This function attains its minimum value when the set of pixels inside the contour have all been classified as shadow by the segmentation procedure.

Using these two energy terms, the posterior distribution of θ given x is:

$$P_{\Theta/X}(\theta/x) = \frac{1}{Z_x}\exp -\underbrace{\{\epsilon_c(\theta,x) + \epsilon_r(\theta,x)\}}_{\epsilon(\theta,x)} \tag{7}$$

$$= \frac{1}{Z_x}\frac{1}{N_{\gamma_\theta^\bullet}N_{\gamma_\theta}}\left(\sum_{s\in\gamma_\theta}\Phi_{S'}(s)\right)\left(\sum_{s\in\gamma_\theta^\bullet}\delta(x_s, e_0)\right), \tag{8}$$

where Z_x is a normalizing constant depending on x only.

3.2 Detection Step

We formulate the detection problem as the search of the *Maximum A Posteriori* (MAP) estimation of θ:

$$\hat{\theta}_{MAP} \in \arg\max_\theta\big\{P_{\Theta/X}(\theta/x)\big\} \tag{9}$$

$$\in \arg\min_\theta \epsilon(\theta, x) \tag{10}$$

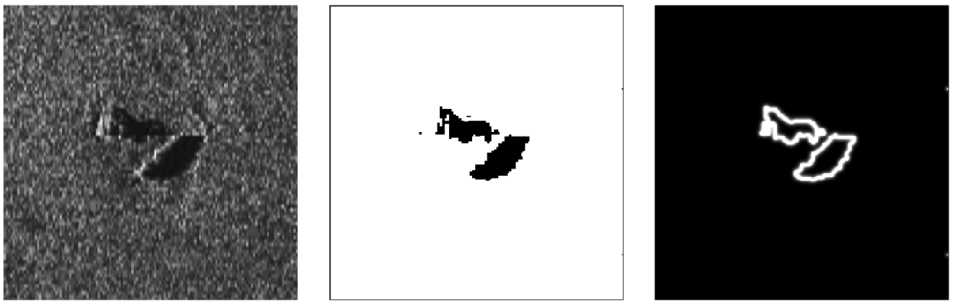

(a) (b) (c)

Fig. 5. (a) Sonar image (image called *rock and object*). (b) Associated Markovian two-class segmentation. (c) Edge potential field with $\sigma = 1$.

This function, $\epsilon(\theta, x)$, is minimal when the deformed template exactly coincides with the edges of x and contains only pixels labeled as *shadow*.

3.3 Classification Step

The resulting value of energy $\epsilon(\hat{\theta}_{MAP}, x)$ is used to measure the degree of fitness of the template with the region of interest and, then, to determine whether the desired object is present or not. If $\epsilon(\hat{\theta}_{MAP}, x)$ is lower than a given threshold, then the desired object is assumed to be present and the final configuration of the deformed template reveals the shape and the location of the detected object; otherwise, we decide that the desired object is not present.

The method can be easily improved in order to retrieve several object-cast shadows looking like the prototype template in the input subimage. In this way, multiple object-cast shadows that are like the prototype template can be localized by using our classification method. Then, we remove the edge in $\Phi_{S'}$ (the edge potential field) of the detected cast shadow shapes and we repeat the same procedure until the value of $\epsilon(\theta, x)$ is sufficiently "large." This procedure prevents the algorithm presented in the following section to always "converge" toward the same object. Nevertheless, in our proposed detection-classification method, this abovementioned procedure is not necessary: When a cast shadow shape is detected as being the one belonging to a manufactured object, the associated sonar subimage is then further analyzed by an expert in order to confirm or to deny this detection. Finally, in the mine war context, the number of no manufactured objects (rocks, ...) is fortunately much larger than manufactured objects!

4 Optimization Problem

The objective function to be maximized in (7) is a complex function with several local extrema over the deformation parameter space. A global search is usually impossible due to the size of the configuration space. Instead, we have implemented and compared three different optimization techniques: a gradient-based method as a local minimization technique; the SA and a GA as global minimization techniques, which are able to escape from local energy minima.

4.1 Gradient-Based Algorithm

This method requires a good initialization of the template, near the true location of the cast shadow shape to be detected. Otherwise, we obtain a suboptimal solution (local minima) and the value of the resulting objective function $\epsilon(\theta, x)$ cannot be exploited to affirm the presence of the desired object.

In order to avoid this difficulty, a solution, proposed in [10], consists of placing the template at evenly spaced positions and in deforming it according a discretized set of orientation, stretch, skew values in the input image. These deformed template configurations can then be used to initialize a deterministic gradient descent algorithm. However, the sampling of template positions and transformation parameters must be chosen judiciously. It should be fine enough not to miss the significant local minima of the energy surface and large enough to avoid high computational requirements.

4.2 Simulated Annealing Algorithm

SA [12] is a stochastic relaxation technique which is based on the analogy to the physical process of annealing a metal: At high temperature, the atoms are randomly distributed. With decreasing temperatures, they tend to arrange themselves in a crystalline state which minimizes the global energy. Using this analogy, the algorithm generates, at random, new configurations of the template by sampling the probability distribution of the system "at temperature T":

$$P_{[T]\Theta/X}(\theta/x) \triangleq \frac{1}{Z(T,x)} \exp\left\{-\frac{\epsilon(\theta,x)}{T}\right\}, \tag{11}$$

where parameter T slowly decreases to 0. More precisely, starting from a prototype template $\theta^{[0]}$, we construct a sequence of template deformations $\theta^{[1]}, \theta^{[2]}, \ldots, \theta^{[k]}$ such that $\lim_{k\to\infty} \theta^{[k]} \in \arg\min \epsilon(\theta, x)$. In our application, we consider the Metropolis algorithm and, for every k, we sequentially update each of the component $\theta_i^{[k]}$ of $\theta^{[k]}$ (i.e., each deformation parameter) in the following manner:

- The algorithm generates a new value for $\theta^{[k]}$ (called $\theta_{new}^{[k]}$) that differs from the precedent value (that we call $\theta_{old}^{[k]}$) only by $\theta_i^{[k]}$, randomly chosen according to uniform distributions over admissible intervals of values.
- Then, $\theta_{new}^{[k]}$ or $\theta_{old}^{[k]}$ is selected with probability $P_{new}^{[k]}$ or $P_{old}^{[k]}$, respectively:

$$P_{new}^{[k]} = \min\left\{\frac{\exp\left\{-\frac{\epsilon(\theta_{new}^{[k]},x)}{T_k}\right\}}{\exp\left\{-\frac{\epsilon(\theta_{old}^{[k]},x)}{T_k}\right\}}, 1\right\} \tag{12}$$

and

$$P_{old}^{[k]} = 1 - P_{new}^{[k]}. \tag{13}$$

Increases of energy can thus be accepted and the algorithm is able to escape from local energy minima. It has been shown [17] that the algorithm converges to a global energy minimum if the temperature at iteration k is:

$$T_k \geq \frac{T_0}{\log(1+k)}, \tag{14}$$

where T_0 is a constant depending on the amount of energy which is necessary to escape local minima. Nevertheless, this condition results in an extremely slow procedure. One way to restrict the number of iterations is to use a geometric temperature schedule [12]:

$$T_k = T_0 \left(\frac{T_f}{T_0}\right)^{\frac{k}{K_{max}}}, \tag{15}$$

where T_0 is the starting temperature, T_f is the final temperature, and K_{max} is the number of iterations.

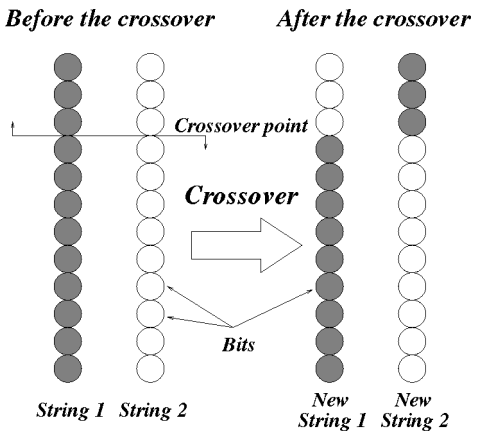

Fig. 6. An example of crossover with the partial exchange of information.

4.3 Genetic Algorithm

Genetic Algorithms (GA) are a class of robust stochastic search and global optimization procedures which mimics the evolution of natural systems [17]. The algorithm acts in an iterative way by allowing parallel evolution in a population of N individuals. Each individual represents a point of the search space and is a candidate solution to the optimization problem. It is represented by a string or *chromosome*, which is composed of a list of L features (corresponding to the L search parameters). The parameters have to be encoded in an appropriate manner. The most common approach is to quantize the parameter values and to binary code them. The appropriateness of the various individuals (the tentative *solution*) to the environment is expressed by a fitness function, which (after the characteristics contained in a chromosome have been decoded) gives a *performance* value to the string.

Genetic search is carried out in a sequence of *generations*. In each generation, a new population of N chromosomes is created by the genetic operators. These operators mimic the biological phenomena of *selection*, *crossover*, and *mutation*. The choice of the solution upon which they are used is dictated by the evolutionary principle of the *survival of the fittest*. The algorithm begins with an initial population of N chromosomes randomly chosen and terminates when either a specified number of iterations has been performed or a maximally fit individual has emerged.

In our application, let us recall that we have to optimize an L-dimensional function ($L = 6$ or $L = 4$ depending on the considered deformable template). Each of the L parameters is quantified on q bits. Therefore, the ith chromosome $[\theta]_i$ is a string of $q \cdot L$ bits length:

$$[\theta]_i = \big(\underbrace{c^i_{11}, c^i_{12}, \ldots, c^i_{1q}}_{[\theta_1]}\ ;\ \underbrace{c^i_{21}, c^i_{22}, \ldots, c^i_{2q}}_{[\theta_2]}\ ;\ \ldots\ ;\ \underbrace{c^i_{L1}, c^i_{L2}, \ldots, c^i_{Lq}}_{[\theta_L]}\big). \tag{16}$$

4.3.1 Fitness Measure

We can easily derive a fitness measure $\mathcal{F}$ (to be maximized) directly from (9) (the energy function ϵ to be minimized).

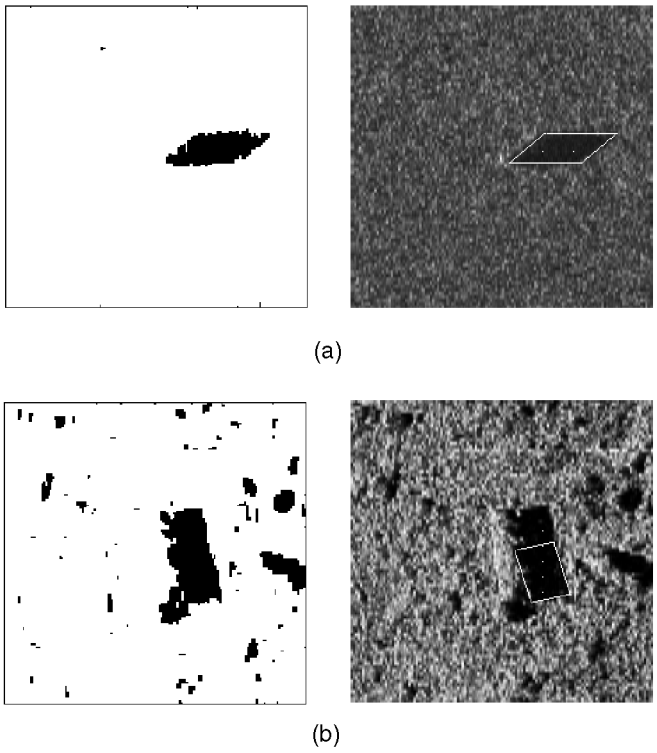

Fig. 7. Template-based detection and classification with a gradient-based local optimization procedure in case of cast shadow of a cylindrical object on a sandy sea bed (image called *object on a sandy sea-bed*) and pebbly sea floor (image called *object on a pebbly sea-bed*). The input two-class segmentation is first shown, then the resulting deformed template is displayed superimposed on the original image. (a) Convergence toward the global minimum: $\epsilon = 0.10$. (b) Convergence to a local minima: $\epsilon = 0.31$.

To turn $\epsilon(\theta, x)$ into a fitness measure for use in genetic algorithm (i.e., one with range $[0, 1]$), one can choose:

$$\mathcal{F}([\theta]_i) = \exp\{-\epsilon([\theta]_i, x)\} \qquad \text{since} \quad \epsilon([\theta]_i, x) \geq 0. \tag{17}$$

The following is the detail of the *selection*, *crossover*, and *mutation* operators. The associated parameters used in our sonar imagery application will be given in Section 5.3.

4.3.2 Selection

Individuals with higher fitness survive and individuals with lower fitness die. Let us assume that, at iteration k, the population of the GA is the set of N chromosomes:

$$\mathrm{POP}^k = \left\{[\theta]^k_1, \ldots, [\theta]^k_N\right\}. \tag{18}$$

Generation of the next population is based on the evaluation of $\mathcal{F}$ for all individuals of POP^k. More precisely, we probabilistically select each chromosome for "reproducing" in the next generation, using their relative fitness:

$$p([\theta]^k_i) = \frac{\mathcal{F}([\theta]^k_i)}{\sum_{j=1}^{N} \mathcal{F}([\theta]^k_j)}. \tag{19}$$

4.3.3 Crossover

A pair of chromosomes is picked up at random and the single-point crossover operator is applied according to a fixed crossover probability. For this operation, a random

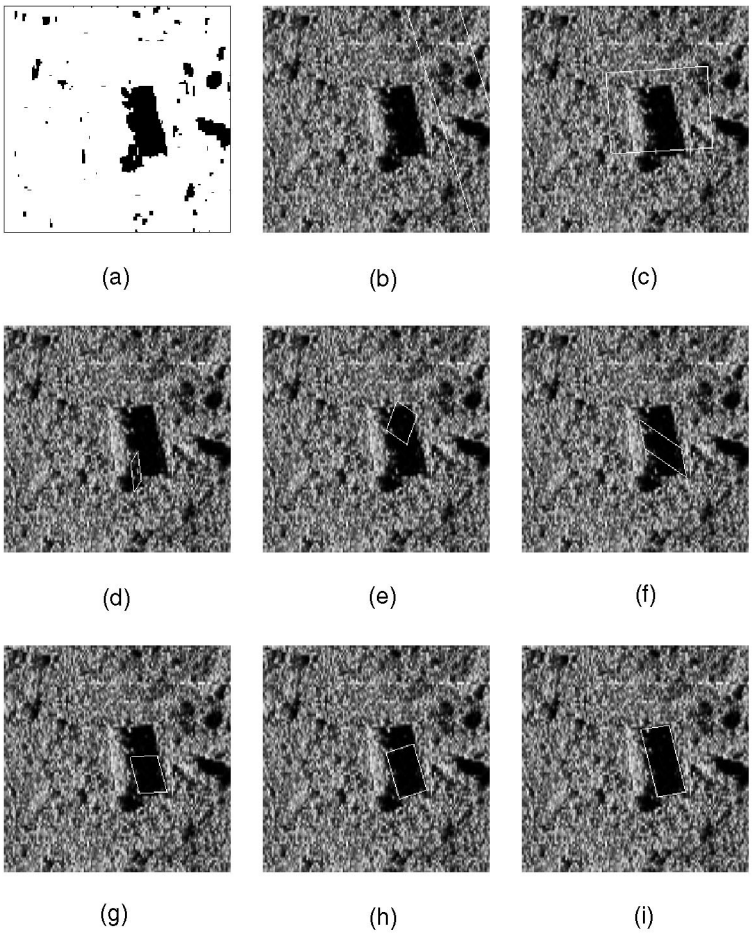

Fig. 8. Evolution of the deformable template during the SA optimization on an image (*object on a pebbly sea-bed*) involving the cast shadows of a cylindrical object on a pebbly sea-floor. (a) Two-class Markovian segmentation of the sonar image presented in (b)-(i). (b) Initial position of the deformed template. (c)-(i) Successive iterations of the simulated annealing procedure. (i) Final segmentation, $\epsilon = 0.13$, leads to classifying the selected region as the cast shadow of a cylindrical manufactured object.

number in the range of 0 to the length Lq of the string is generated. This is called the crossover point. The portions of two strings lying to the right of the crossover point are interchanged to yield two new strings, as shown in Fig. 6.

4.3.4 Mutation

Mutation consists of considering in turn each bit of a given chromosome and changing its value with a predefined low probability called the mutation rate.

In order to prevent premature convergence [17] and to speed up the convergence rate, we have developed three strategies and we have combined them:

1. The first one is an elite-preservation strategy [17]: The individual with the highest fitness always survives to be an individual of the next generation.
2. The second strategy (called hybrid GA [17]) consists of associating the genetic search with a local optimization technique. In each generation, a percentage of the best individuals are used to initialize a gradient ascent technique. Therefore, these best individuals explore local neighborhoods in the parameter space to find a point of higher fitness.
3. In order to improve the results and the robustness of the GA, we propose a third modification reminiscent to SA [18]. The fitness function $\mathcal{F}$ at iteration k is defined as follows:

$$\mathcal{F}^k([\theta]_i) = \exp\left\{-\frac{1}{T_k}\epsilon([\theta]_i, x)\right\} \tag{20}$$

with $T_k = T_0 a^k$ and $a<1$. At the beginning of the genetic search procedure, $T_k>1$ and the optimization procedure exploits a smooth version of the energy function ϵ. This smooth energy function has fewer spurious local minima, which helps the genetic procedure to maintain a good diversity in the population and to avoid a premature convergence toward a suboptimal solution (corresponding to an important secondary minima). For $T_k=1$, the genetic search is carried out with the real cost function ϵ. At the end of the procedure, $T_k<1$, the fitness measure falls off rapidly with increasing cost. This allows us to maintain a good competition between individuals located near the global optimum and to localize precisely the global extrema. This method is similar to the cooling temperature

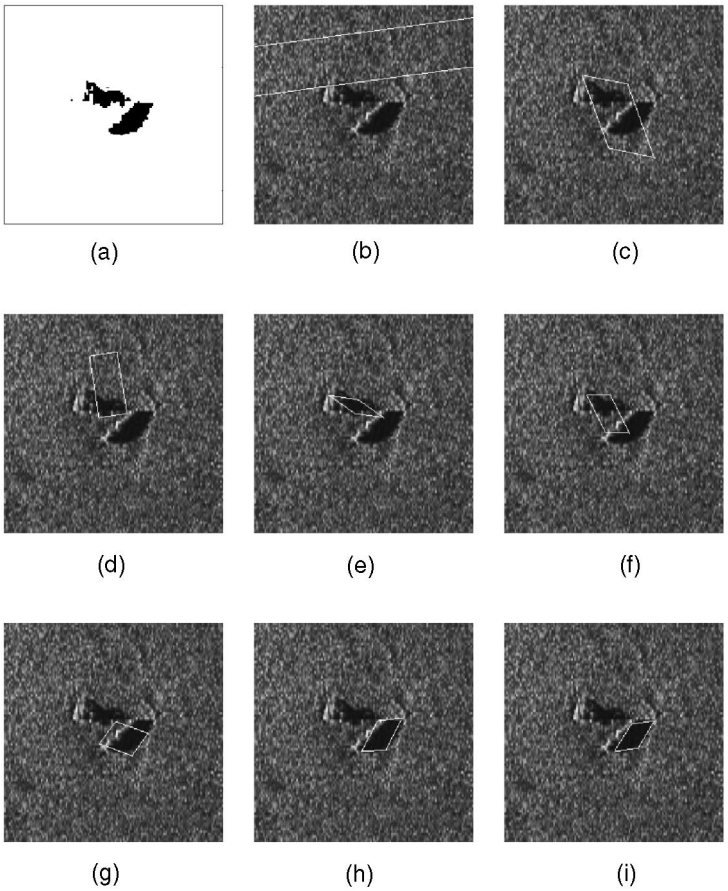

Fig. 9. Evolution of the deformable template during the SA optimization on an image (*rock and object*) involving the cast shadow of a rock and a cylindrical object. (a) Two-class Markovian segmentation of the sonar image presented in (b)-(i). (b) Initial position of the deformed template. (c)-(i) Successive iterations of the simulated annealing procedure. (i) Final segmentation, $\epsilon = 0.19$, leads to classifying the selected region as the cast shadow of a cylindrical manufactured object.

schedule proposed in the simulated annealing procedure. In our application, these three strategies are used together in an efficient way. We call this algorithm a hybrid genetic algorithm with an elitist strategy and a cooling temperature schedule.

5 Experimental Results

In order to distinguish natural from man-made objects, we have to search the presence or not of both templates. For the classification step, we use the following decision rules:

- If $\epsilon < 0.2$, we decide that the image contains an object whose cast shadow shape is similar to the template.
- If $0.20 < \epsilon < 0.23$, a doubt exists. A human expert is indispensable to classify these objects.

TABLE 1
Minima Obtained with the Different Optimization Procedures for Different Sonar Images

	Image		
optimization	*rock and object*	*object on a sandy sea bed*	*object on a pebbly sea bed*
Gradient-based	$\epsilon = 0.47$	$\epsilon = 0.10$	$\epsilon = 0.31$
SA	$\epsilon = 0.19$	$\epsilon = 0.13$	$\epsilon = 0.13$
GA	$\epsilon = 0.17$	$\epsilon = 0.10$	$\epsilon = 0.15$

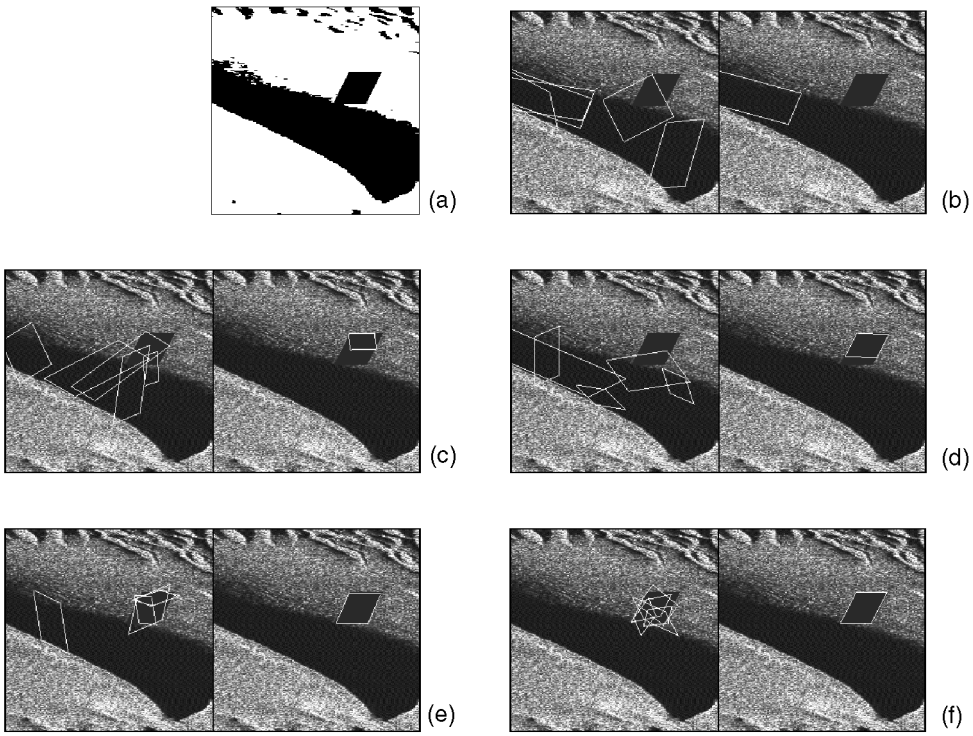

Fig. 10. Successive generations of the genetic search. This sonar image contains a synthetic shadow shape of a cylindrical object partially occluded by a dune of sand cast shadow. (a) Two-class Markovian segmentation of the sonar image. (b)-(f) Best 5 percent deformed templates before the gradient ascent (on the left) and the best resulting template (on the right). GA optimization after (b) 1, (c) 2, (d) 4, (e) 16, (f) 30 generations. Accurate and reliable detection of the cylindrical object-cast shadow is obtained ($\epsilon = 0.06$).

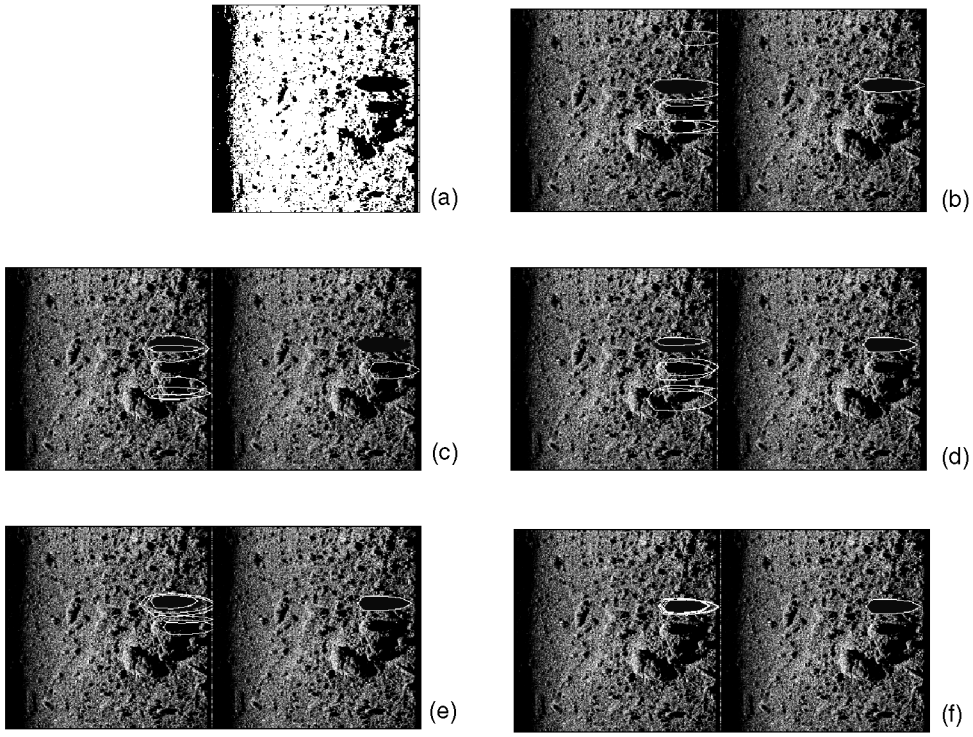

Fig. 11. Successive generations of the genetic search. This sonar image shows the synthetic shadow shape of a spherical object occluded by several rock cast shadows. (a) Two-class Markovian segmentation of the sonar image. (b)-(f) Best 5 percent deformed templates before the gradient ascent (on the left) and the best resulting template (on the right). GA optimization after (b) 1, (c) 4, (d) 6, (e) 8, (f) 24 generations. Accurate and reliable detection of the spherical object-cast shadow is obtained ($\epsilon = 0.10$).

- If $\epsilon > 0.23$, we decide that the searched object is not present in the input image.

These different threshold values have been chosen empirically after a set of experiments from our database

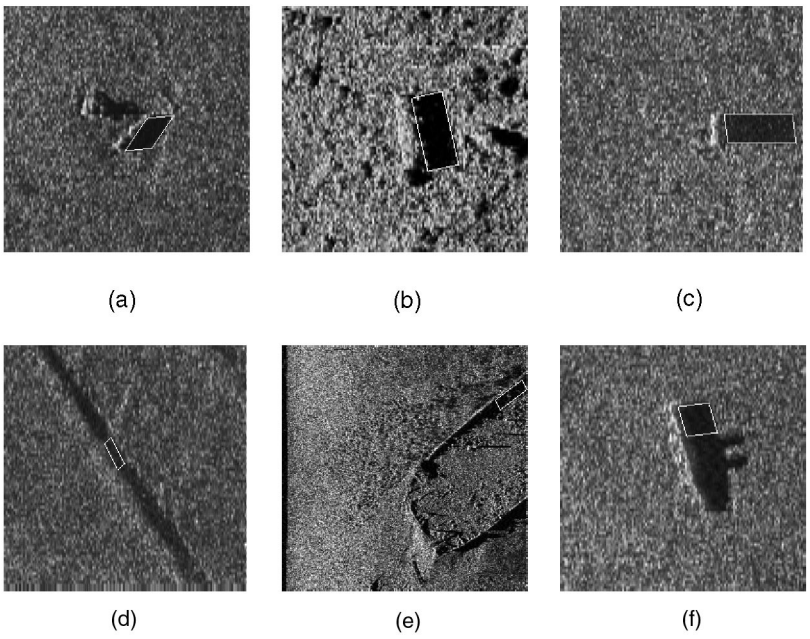

Fig. 12. The parallelogram template and the low value obtained (with the genetic search) for ϵ ($\epsilon < 0.2$) allow us to classify these shadows as "manufactured object-cast shadow." (a), (b), (c) Different cylindrical objects: $\epsilon = 0.17$, $\epsilon = 0.15$, and $\epsilon = 0.14$, respectively. (d) Pipe-line: $\epsilon = 0.12$. (e) Wreck: $\epsilon = 0.15$. (f) Trolley: $\epsilon = 0.2$.

of 100 real sonar images (containing natural or manufactured objects of different nature) and with the optimization procedure ensuring the global minimum (i.e., with the genetic search). As we will show in the following, this decision rule leads, for our application, to a good classification rate.

The proposed deformable template-based detection and the classification scheme have been now applied to several real and synthesized sonar images containing natural or manufactured objects. These experiments have been carried out with the different optimization procedures previously presented. The efficiency of each method is discussed and experimental results are compared.

5.1 Gradient-Based Optimization

First experiments have been carried out with the gradient-based optimization and the sampling strategy described in Section 4.1. In our application, we considered a number of possible initializations by selecting five values of each parameter (yielding, respectively, 5^4 possible shapes of the first kind and 5^2 of the second kind) and different locations evenly spaced within shadow regions.

Fig. 7 shows the cast shadow created by a cylindrical object lying on a sandy sea floor and on a pebbly sea floor, respectively. Let us note that, for the latter case, the cylinder object cast shadow occludes a number of rock shadows and the background is rather cluttered. For each case, we present the resulting deformed template and we indicate the corresponding energy value. In the first example, we can see that the outline of the cast shadow shape is accurately recovered and the low value of the energy function allows us to correctly classify this shadow shape as a cylindrical object-cast shadow. However, in the second case, the energy function is too complex (i.e., many local minima due to the complex background and the different occlusions) and/or the initialization given to the gradient-based procedure is not good enough to ensure a correct detection. We obtain a suboptimal solution (local minima) and the value of the resulting objective function does not allow us to recognize the presence of a manufactured object in this sonar image.

5.2 Simulated Annealing Optimization

A second set of experiments have been conducted using the SA optimization scheme with a geometrical temperature schedule and the following control parameters: $T_0 = 2$, $T_f = 0.005$, $K_{max} = 15,000$. Tests have shown that this optimization procedure is very sensitive to the parameters of the cooling schedule. In our application, these parameters have been chosen empirically in order to get good convergence in all tested case (around 100 sonar pictures).

Fig. 8 illustrates the evolution of the (parallelogram) template during the SA optimization on the same image as in Fig. 7b. In the beginning, the temperature is relatively high, then the algorithm explores the space of template parameters even if the corresponding deformed templates do not satisfy the constraints and have a relatively high energy. As the temperature decreases, the constraints become satisfied, the outline of the template gets closer to the edges of the region of interest, and the energy converges toward the global minimum. Then, the low value of the energy ($\epsilon = 0.13$ compared to $\epsilon = 0.3$) obtained by gradient-based technique allows us to classify this region of interest as the cast shadow of a cylindrical object. In Fig. 9, the detected region of interest extracted by the parallelogram template corresponds well to the manufactured object (cylindrical object) and the low value of ϵ allows us to classify it as the cast shadow of a cylindrical object.

This procedure ensures a good detection and correct classification rate. Nevertheless, one of the major drawbacks

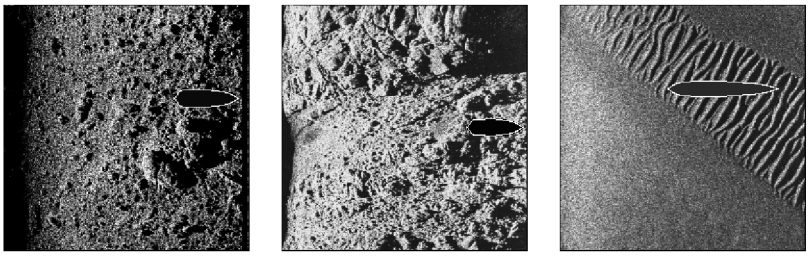

Fig. 13. The cubic B-spline template and the low value obtained (with the genetic search) for ϵ ($\epsilon < 0.2$) allows us to classify these shadows as "spherical object-cast shadow." (a) $\epsilon = 0.04$. (b) $\epsilon = 0.15$. (c) $\epsilon = 0.19$.

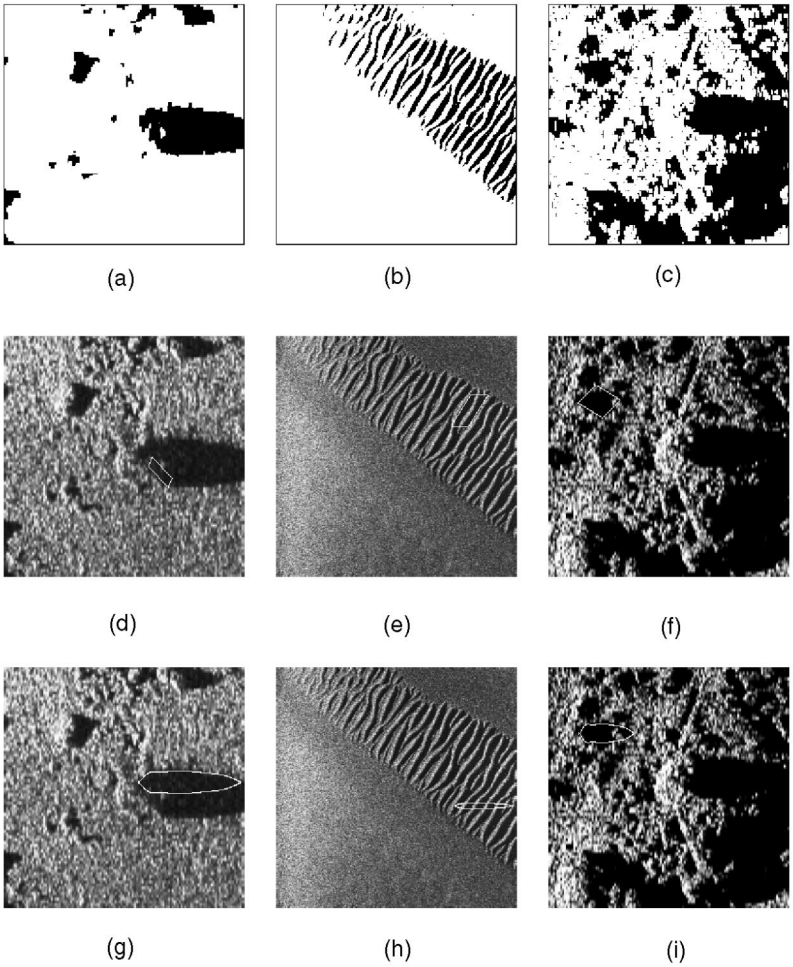

Fig. 14. The values of ϵ (> 0.2) (obtained with the genetic search) for both templates are sufficiently large so that we can reject the hypothesis of a manufactured or spherical object present in these images. (a)-(c) Markovian segmentation of the sonar images. (d) $\epsilon = 0.40$. (e) $\epsilon = 0.41$. (f) $\epsilon = 0.24$. (g) $\epsilon = 0.55$. (h) $\epsilon = 0.57$. (i) $\epsilon = 0.38$.

of this optimization procedure is its high computational load. It takes about seven minutes on a 43P IBM (120 MHz) workstation, whereas about one minute is necessary for the gradient-based optimization previously described. However, the K_{max} parameter should be chosen less than $15,000$, but it seemed that this maximum iteration number was reasonable for such robustness on a large database. Moreover, the final temperature is very low ($T_f = 0.005$): This ensures a quasi-deterministic search at the end of the stochastic procedure. This is why it is not necessary to apply a deterministic search at the end of the simulated annealing-based optimization procedure to further improve the optimization result. These two reasons explain the large computing time required for the SA algorithm.

5.3 Genetic Optimization

These last experiments have been carried out with the hybrid genetic algorithm using the elitist strategy and the cooling temperature schedule described in Section 4.3. Tests have shown that this optimization procedure was not very sensitive to the control parameters. In our application, these parameters are the following: population size = 100,

crossover rate = 0.8, mutation rate = 0.008, maximum number of generations = 150. Some tests have shown that the genetic algorithm-based optimization procedure is not very sensitive to mutation parameter if it is contained within the range $[0.001, 0.01]$, as proposed by Goldberg [17]. At each generation, we select 5 percent of the best individuals for the hybridization with the local optimization technique and the cooling schedule parameters are $T_0 = 2$ and $a = 0.99$.

Our GA takes about 20-120 generations to converge to the true solution. In fact, the convergence rate can vary significantly depending on the complexity of the objective function ϵ to be minimized (or the complexity of the input image). The optimization procedure takes between 10 seconds and 35 seconds on a 43P IBM workstation. In all processed cases, we obtain the same good results far more quickly than those provided by the simulated annealing (see Table 1).

Fig. 10 (a real sonar image on which a synthetic shadow shape of a cylindrical object has been added) illustrates the best deformed template and the best 5 percent set of templates before the gradient ascent technique for successive iterations or generations of the genetic search. We can see that this method is efficient even if the cast shadow shape is partially occluded. Fig. 11 shows the detection and the classification of a synthetic cast shadow shape associated with a spherical object added on a real sonar image.

Figs. 12, 13, 14 show a few examples of classification results from our database. Geometric shape, i.e., manufactured objects, are well-detected, such as the geometric part of a wreck (Fig. 12e), a section of a pipe-line (Fig. 12d), a trolley (Fig. 12f), and different cylindrical objects (Fig. 12a Fig. 12b, Fig. 12c). In the same way, spherical objects (Fig. 13) are well detected even if the cast shadow shape is partially occluded. Fig. 14 shows several natural objects and the associated values of the objective function $\epsilon(\theta, x)$.

6 Conclusion

In this paper, we have developed a novel and robust algorithm to distinguish, from sonar images, man-made objects from natural objects lying on the sea-bed. The proposed method enables us to distinguish natural objects from manufactured objects lying on the sea-bed. The whole paper is presented with this intention.[1] We have stated the detection and the classification issues within a statistical setting and we have shown that this problem can be handled as an equivalent energy minimization problem. The energy function is minimized using a stochastic genetic search combined with a local optimization technique and a cooling temperature schedule. This optimization procedure is fast, robust, simple, and well-suited to our application compared to other minimization techniques such as gradient-based method or the simulated annealing algorithm. The proposed scheme appears as an original alternative to feature-based matching methods, and remains very efficient in the case of complex cluttered backgrounds and occlusion phenomena between several object cast shadows. This method has been applied to a number of real sonar images; the obtained results demonstrate its efficiency and robustness. This scheme is fast and robust enough to allow automatic processing of massive amounts of data. Besides, this method can be easily improved in order to retrieve several object cast shadows that are like the prototype template in the input subimage. In that prospect, multiple object-cast shadows looking like the same prototype template can be localized by using our classification method. Then, we remove the edge in $\Phi_{S'}$ of the detected cast shadow shapes and we repeat the same procedure till the value of ϵ is sufficiently large.

1. In a military context, this method may also be used to detect and to localize cylindrical or spherical mines lying on the sea-floor. It is our applicative context. Unfortunately, confidentiality reasons prevent us from providing too much information on the application.

Acknowledgments

The authors thank GESMA (Group d'Étude Sous Marine de l'Atlantique, Brest, France) for providing numerous real sonar pictures and DGA (Direction Générale pour l'Armement, French Ministry of Defense) for partial financial support of this work (student grant).

References

[1] P. Galerne, K. Yao, and G. Burel, "Objects Classification Using Neural Network in Sonar Imagery," *Proc. European Symp. Lasers and Optics in Manufacturing,* vol. 1, pp. 306-311, June 1997.

[2] J.C. Hyland and G.J. Dobeck, "Sea Mine Detection and Classification Using Side-Looking Sonar," *Detection Technologies for Mines and Minelike Targets,* vol. SPIE 2496, pp. 442-453, Apr. 1995.

[3] F. Schmitt, M. Mignotte, C. Collet, and P. Thourel, "Estimation of Noise Parameters on Sonar Images," *Signal and Image Processing,* vol. SPIE 2823, pp. 1-12, Aug. 1996.

[4] J. Besag, "On the Statistical Analysis of Dirty Pictures," *J. Royal Statistical Soc.,* vol. B-48, pp. 259-302, 1986.

[5] M. Mignotte, C. Collet, P. Pérez, and P. Bouthemy, "Unsupervised Markovian Segmentation of Sonar Images," *Proc. Int'l Conf. Acoustics, Speech, and Signal Processing,* vol. 4, pp. 2,781-2,785, May 1997.

[6] C. Regazzoni, F. Arduini, and G. Vernazza, "A Multilevel GMRF-Based Approach to Image Segmentation and Restoration," *Signal Processing,* vol. 34, pp. 43-67, 1993.

[7] U. Grenander and M. Keenan, "Towards Automated Image Understanding," *Advances in Applied Statistics,* vol. 16, pp. 89-103, 1993.

[8] K. Kluge and S. Lakshmanan, "Lane Boundary Detection Using Deformable Templates: Effects of Image Subsampling on Detected Lane Edges," *Proc. Asian Conf. Computer Vision,* pp. 141-145, Dec. 1995.

[9] S. Lakshmanan and D. Grimmer, "A Deformable Template Approach to Detecting Straight Edges in Radar Images," *IEEE Trans. Pattern Analysis and Machine Intelligence,* vol. 18, no. 4, pp. 438-443, Apr. 1996.

[10] A.K. Jain, Y. Zhong, and S. Lakshmanan, "Object Matching Using Deformable Templates," *IEEE Trans. Pattern Analysis and Machine Intelligence,* vol. 18, no. 3, pp. 267-278, Mar. 1996.

[11] M.P. Dubuisson Jolly, S. Lakshmanan, and A.K. Jain, "Vehicle Segmentation and Classification Using Deformable Templates," *IEEE Trans. Pattern Analysis and Machine Intelligence,* vol. 18, no. 3, pp. 293-308, Mar. 1996.

[12] S. Geman and D. Geman, "Stochastic Relaxation, Gibbs Distributions and the Bayesian Restoration of Images," *IEEE Trans. Pattern Analysis and Machine Intelligence,* vol. 6, no. 6, pp. 721-741, Nov. 1984.

[13] C. Kervrann and F. Heitz, "Statistical Model-Based Segmentation of Deformable Motion," *Proc. Int'l Conf. Image Processing,* pp. 937-940, 1996.

[14] Y. Nakazawa, T. Komatsu, and T. Saito, "A Robust Object-Specified Active Contour Model for Tracking Smoothly Deformable Line-Features and Its Application to Outdoor Moving Image Processing," *Proc. Int'l Conf. Image Processing,* pp. 689-692, Sept. 1996.

[15] Y. Fisher, *Fractal Image Compression: Theory and Application.* Springer-Verlag, 1995.
[16] J.W. Goodman, "Some Fundamental Properties of Speckle," *J. Optical Soc. Am.,* vol. 66, no. 11, pp. 1,145-1,150, Nov. 1976.
[17] D.E Goldberg, *Genetic Algorithm.* Addison Wesley, 1989.
[18] M. Mignotte, C. Collet, P. Pérez, and P. Bouthemy, "Statistical Model and Genetic Optimization: Application to Pattern Detection in Sonar Images," *Proc. 23rd IEEE Int'l Conf. Acoustics, Speech, and Signal Processing—ICASSP '98,* vol. 5, pp. 2,541-2,544, May 1998.

Max Mignotte received the DEA (postgraduate degree) in digital signal, image, and speech processing from the Institut National Polytechnique of Grenoble, France, in 1993, and the PhD degree in digital signal and image processing from the University of Bretagne Occidentale, France in 1998 (thesis achieved at the laboratory GTS (Groupe de Traitement du Signal) of the French Naval Academy). He is currently an INRIA post-doctoral fellow at Montreal University (DIRO), Quebec, Canada. His current research interests include Bayesian inference, image segmentation (hierarchical Markovian models or deformable models), parameters estimation, tracking, classification, deconvolution/restoration, and optimization problems in sonar or medical images.

Christophe Collet graduated from the Université Paris-Sud Orsay in 1989 (DEA in Signal Processing) and received the PhD degree in image analysis from the University of Toulon, France, in 1992. His thesis research was carried out at the Ecole Nationale Supérieure des Télécom. de Bretagne (ENST-Br) and at the French Naval Academy. He is currently "maître de conférences" at the French Naval Academy and chairman of the laboratory GTS "Groupe de Traitement du Signal" since 1994. The line of research of the GTS laboratory concerns signal and image processing for underwater acoustic applications. His main research interests include image modeling, Markovian segmentation, Bayesian estimation, pattern recognition, texture analysis, statistical optimization techniques for image analysis. The main applications deduced from this research framework deal with motion segmentation of infrared image sequences, segmentation of seafloor for man-made pattern classification, multispectral segmentation of SPOT images.

Patrick Pérez graduated from the Ecole Centrale Paris, France, in 1990. He received the PhD degree in signal processing and telecom. from the University of Rennes, France, in 1993. He spent one year as an INRIA postdoctoral fellow at Brown University (Department of Applied Mathematics). He now holds a full-time research position at the INRIA center in Rennes. His research interests include statistical and/or hierarchical models for large inverse problems in image analysis, with a particular focus on motion analysis issues (detection, segmentation, and estimation of the apparent motion, tracking, analysis of elastic and fluid motions, etc.).

Patrick Bouthemy graduated from the Ecole Nationale Superieure des Telecommunications, Paris, in 1980, and received the PhD degree in computer science from the University of Rennes, France, in 1982. From December 1982 until February 1984, he was employed by INRS-Telecommunications, Montreal, P.Q., Canada, in the Department of Visual Communications. Since April 1984, he has been with INRIA at IRISA in Rennes. He is currently "Directeur de Recherche" INRIA and head of the Vista project. His major research interests are concerned with image sequence analysis: 2D motion analysis (rigid motion and deformable motion), statistical models for image sequence processing (MRF models, robust estimation, Bayesian estimation), dynamic scene interpretation, active vision, video indexing. He is an associate editor of the *IEEE Transactions on Image Processing*.